Coagulation and Fragmentation: The Variation of Shear Rate and the Time Lag for Attainment of Steady State

Patrick T. Spicer, Sotiris E. Pratsinis,* and Michael D. Trennepohl

Department of Chemical Engineering, University of Cincinnati, Cincinnati, Ohio 45221-0171

Gabrie H. M. Meesters

Genencor International B.V., 2600 AP Delft, The Netherlands

The dynamic behavior and the attainment of steady state by a flocculating suspension in a stirred tank are evaluated using a population balance model. At long times, shear-induced coagulation and fragmentation reach a steady state, resulting in a particle size distribution (PSD) that is invariant (self-preserving) with respect to shear. The geometric standard deviations, σ_g, of the self-preserving number or volume PSDs are 2.22 or 1.79, respectively, for the employed coagulation and fragmentation rates of flocculation. The time required to reach a steady-state PSD (time lag) is determined as a function of a dimensionless group comprised of the relative rates of coagulation and fragmentation. The effect of the omnipresent variable shear rate in stirred tanks during shear-induced flocculation is investigated through a sinusoidal function of the spatially averaged velocity gradient. Increasing the amplitude of the shear rate fluctuation decreases the steady-state mass mean floc size, the maximum σ_g, and the time lag for attainment of steady state. The asymptotic (self-preserving) σ_g is not affected by the shear rate amplitude provided that >99% of the primary particles have grown to larger sizes.

Introduction

Many industrial processes involve coagulation and fragmentation of the suspended phase in stirred tanks. Examples include polymerization (Blatz and Tobolsky, 1945), liquid−liquid dispersion (Coulaloglou and Tavlarides, 1977), emulsification (Danov et al., 1994), and flocculation (Lu and Spielman, 1985). An important design and control parameter in these processes is the size distribution of the suspended particles. In most practical systems, a steady state or equilibrium is reached between coagulation and fragmentation after a certain time (time lag) and the particle size distribution (PSD) no longer changes. This time lag determines the process requirements (i.e., batch time, power input, etc.) of a flocculation process.

Experimental studies have shown that the spatially averaged shear rate varies significantly throughout a stirred tank (Cutter, 1966; Sprow, 1967). Realistic descriptions of flocculation account for the high shear region around the impeller (impeller zone) and various bulk regions above and below the impeller with significantly lower relative shear rates. Koh et al. (1984, 1987), for example, coupled multicompartmental models of a stirred tank with the population balance equations to fit data on scheelite flocculation but considered only coagulation with no fragmentation. A two-compartment model gave results as good as those of models using a larger number of compartments. Kim and Glasgow (1987) developed a Monte Carlo model of coagulation and fragmentation assuming random movement/shearing of particles, a size-dependent fragmentation rate, and a time step based on the frequency of exposure to the impeller zone. Few comparisons with experimental data were performed, and good agreement with the evolution of the average size of kaolin−polymer flocs was reported (Kim and Glasgow, 1987). Kusters (1991) combined a six-compartment stirred-tank model with analytical velocity profiles to track particle residence times in each compartment. He derived expressions for the frequency of successful coagulation and fragmentation and predicted the evolution of the average floc size well. Recently, Seckler et al. (1995) studied stirred-tank hydrodynamics using computational fluid dynamic (CFD) models coupled with a moment model of the particle size distribution during precipitation. The model identified specific regions of particle formation in a precipitation reactor.

The shape of the asymptotic PSD affects the efficiency of a solids removal process. Theoretical investigations have indicated that pure shear-induced coagulation does not result in a self-preserving PSD (Swift and Friedlander, 1964; Pulvermacker and Ruckenstein, 1974), that is, a PSD whose shape scales with the average particle size. Theoretical (Tambo and Watanabe, 1979; Family et al., 1986; Meakin, 1988; Cohen, 1992; Spicer and Pratsinis, 1996a) and experimental (Spicer and Pratsinis, 1996b) studies have shown, however, that the steady-state PSD from coagulation−fragmentation processes is self-preserving with respect to process conditions. When self-similarity is observed, the individual coagulation and fragmentation rates in the suspension may be determined by deconvolution of the steady-state PSD (Narsimhan et al., 1980; Wright and Ramkrishna, 1994).

The time lag for attainment of steady state by a coagulation−fragmentation process has been investigated previously (Blatz and Tobolsky, 1945; Peled et al., 1995), but models incorporating realistic, size-dependent rate expressions have not been used. In addition, few studies have been carried out on the effect of heterogeneous flow conditions on a flocculating particle size distribution. The objective of this study is to determine the time lag for attainment of steady state by coagulation and fragmentation using rates commonly encountered during flocculation (Lu and Spielman, 1985). To meet this goal, a population balance model is used

* To whom correspondence should be addressed. Phone: (513)-556-2761. FAX: (513)-556-3473. E-mail: spratsin@alpha.che.uc.edu.

S0888-5885(95)00786-X CCC: $12.00

(Spicer and Pratsinis, 1996a) that has successfully simulated experimental data of polystyrene particle flocculation (Oles, 1992). Furthermore, the effect of constant and varying shear rates on the time lag and the polydispersity of the steady-state PSD is investigated and related to controllable process variables through dimensionless groups.

Theory

The dynamic behavior of the particle size distribution undergoing simultaneous coagulation and fragmentation is given by (Friedlander, 1977; Kusters et al., 1993):

$$\frac{dn_i}{dt} = \frac{1}{2}\sum_{j+k=i} \alpha\beta(u_j,u_k)\, n_j n_k - n_i \sum_{k=1}^{max} \alpha\beta(u_k,u_i)\, n_k - S_i n_i + \sum_{j=1}^{max} \gamma_{i,j} S_j n_j \quad (1)$$

where n_i is the number concentration of flocs of size i (meaning that a single floc contains i primary particles). The first term on the right-hand side (RHS) of eq 1 represents the formation of particles comprised of i primary particles by collisions of smaller j- and k-sized particles. The second RHS term denotes the loss of particles of size i by collision with particles of any other size. The third RHS term describes the loss of particles of size i by fragmentation, and the fourth RHS term describes the formation of particles of size i by the fragmentation of larger particles. The index max represents the largest particle size. Equation 1 is the discrete form of the population balance equation, that is, it describes the change in number concentration of each individual particle size. Thus, in order to model the evolution of the detailed particle size distribution during flocculation, the solution of an enormous number of differential equations would be required using a discrete model. To ease computations, the particle size distribution is divided into size classes or sections.

Equations are written describing the change in particle number concentration in each section based on Hounslow et al. (1988) and Spicer and Pratsinis (1996a):

$$\frac{dN_i}{dt} = \sum_{j=1}^{i-2} 2^{j-i+1}\alpha\beta_{i-1,j}N_{i-1}N_j + \frac{1}{2}\alpha\beta_{i-1,i-1}N_{i-1}^2 - N_i\sum_{j=1}^{i-1} 2^{j-i}\alpha\beta_{i,j}N_j - N_i\sum_{j=i}^{i\,max}\alpha\beta_{i,j}N_j - S_iN_i + \sum_{j=i}^{i\,max}\Gamma_{i,j}S_jN_j \quad (2)$$

where N_i is the number concentration of flocs of size class i (meaning that a single floc contains $1.5 \times 2^{i-1}$ primary particles), α is the collision efficiency for coagulation, $\beta_{i,k}$ is the collision frequency for particles of size class i and k with characteristic volumes v_i and v_k, S_i is the fragmentation rate of flocs of volume v_i, and $\Gamma_{i,j}$ is the breakage distribution function defining the volume fraction of the fragments of size i coming from j-sized particles. The index i max is the number of sections used in the model (here i max = 30).

The collision frequency for turbulent shear-induced coagulation, in the absence of viscous retardation and floc structural effects, is (Saffman and Turner, 1956)

$$\beta_{i,j} = \beta(v_i,v_j) = 0.31G(v_i^{1/3} + v_j^{1/3})^3 \quad (3)$$

where G is the spatially averaged shear rate (Clark, 1985) given for fluctuating shear rates by:

$$G = G' + \omega \sin(t) \quad (4)$$

G' is a constant (e.g., 50 s^{-1}) and ω is the maximum magnitude of the fluctuation in G. A range of ω values were examined here (ω = 0, 30, 40, 50 s^{-1}).

The fragmentation rate is a function of particle volume (Pandya and Spielman, 1982):

$$S_i = Av_i^a \quad (5)$$

where $a = {}^1/_3$ (Boadway, 1978; Peng and Williams, 1994), consistent with the theoretical expectation that breakage rate is proportional to the floc diameter. The parameter A is the breakage rate coefficient for shear-induced fragmentation (Pandya and Spielman, 1982):

$$A = A'G^y \quad (6)$$

where y is a constant inversely proportional to the floc strength and A' is a proportionality constant that is determined experimentally. The value of $y = 1.6$ was used in all calculations corresponding to kaolin−polymer and polystyrene flocs (Pandya and Spielman, 1982; Spicer and Pratsinis, 1996a). The constant A' affects the relative strength of fragmentation relative to coagulation and a value of 0.0047 is used here (Oles, 1992; Spicer and Pratsinis, 1996a).

For all calculations, binary breakage was assumed (Spicer and Pratsinis, 1996a):

$$\Gamma_{i,j} = v_j/v_i, \quad \text{for } j = i+1; \qquad = 0, \quad \text{otherwise} \quad (7)$$

Equations 3−7 were substituted into eq 2, and the sectional model was solved numerically using DGEAR, an ordinary differential equation solver (IMSL, 1989).

The behavior of a coagulation−fragmentation system is a function of the relative significance of the rates of coagulation and fragmentation (Blatz and Tobolsky, 1945). As a result, it is convenient to define a dimensionless group that characterizes the relative significance of coagulation versus fragmentation, CF:

$$\mathrm{CF} = S_0 v_0/\phi\beta_{0,0} \quad (8)$$

where ϕ is the volume fraction of suspended particles, v_0 is the volume of a primary particle, and $\beta_{0,0}$ and S_0 are obtained by substituting v_0 into eqs 3 and 5, respectively.

Results and Discussion

Unless stated otherwise, all calculations were carried out for $G = 50\ s^{-1}$, $\alpha = 1$, $\omega = 0$, $A' = 0.0047$, $y = 1.6$, initial diameter $d_0 = 2.17\ \mu m$ (corresponding to an initial volume of $v_0 = 5.35\ \mu m^3$), and initial number concentration $N_1 = 9.3 \times 10^6\ cm^{-3}$ (Oles, 1992; Spicer and Pratsinis, 1996a). The model was validated by comparison with analytical solutions for the case of pure coagulation with a size-dependent kernel (Golovin, 1963), pure fragmentation (Williams, 1990), and the combined case (Blatz and Tobolsky, 1945). At all conditions excellent agreement between the numerical and analytical solutions was obtained (Spicer and Pratsinis, 1996a).

Development of the Steady-State Floc Size Distribution. Figure 1 shows the evolution of the initially

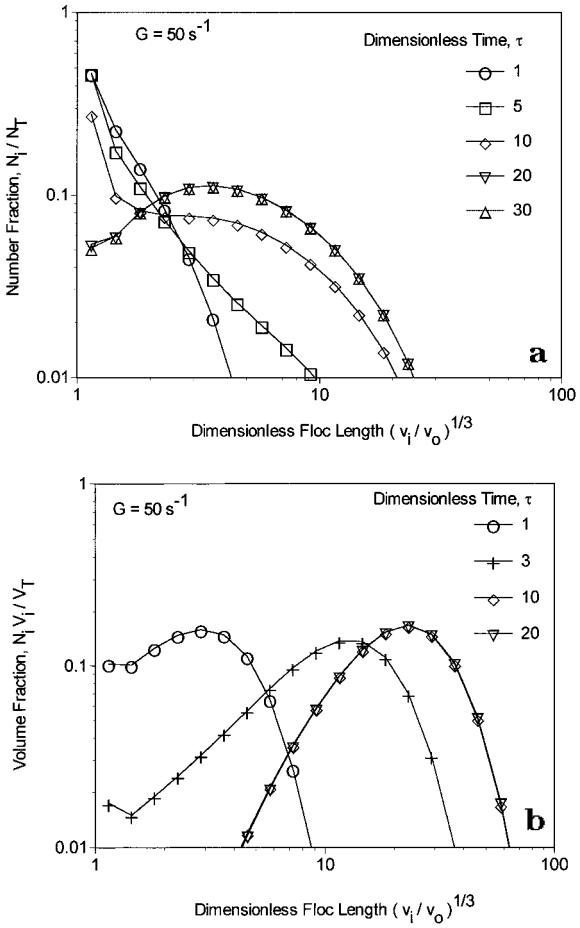

Figure 1. Evolution of the (a) number- and (b) volume-based particle size distributions during shear-induced flocculation at initial conditions $N_1 = 9.3 \times 10^6$ cm^{-3}, $d_1 = 2.17$ μm, $G = 50$ s^{-1}, $\alpha = 1$, $A' = 0.0047$, and $y = 1.6$.

monodisperse particle size distribution as a function of dimensionless time, $\tau = G\phi t$ (Oles, 1992). Initially, growth is slow as the small primary particles collide and form larger ones. Figure 1a shows the evolution of the number distribution. After 1τ, the distribution remains in the first few size classes. After 10τ, an additional, bell-shaped mode forms and the primary particle size class is further depleted. Fragmentation prevents further growth of the larger mode, and these particles serve as collectors of fines (primaries); accelerating the depletion of the primary particles until after 20τ, the distribution no longer changes (e.g., at 30τ). It is worth noting that the primary particles constitute a large (number) fraction, $N_{1ss} = 5\%$, of the steady-state size distribution.

Figure 1b shows the evolution of the volume distribution as a function of τ. Similar to Figure 1a, the initially monodisperse distribution grows into the larger size sections, forming a bell-shaped mode after 1τ. After 10τ, the distribution is indistinguishable from that at 15τ, and steady state is attained in about half the time required for the number-based distribution. The steady-state volume-based PSD is attained much faster than the number-based distribution because the primary particles do not contribute significantly to the former PSD.

Effect of Shear Rate on the Attainment of Steady State. The geometric standard deviation of the floc size distribution, σ_g, quantitatively characterizes the width of the distribution (Hinds, 1982). Figure 2 shows the evolution of σ_g for various shear rates, G ($\omega = 0$). After

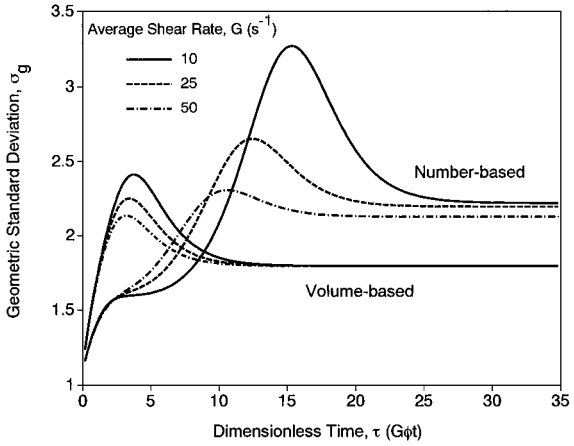

Figure 2. Evolution of the number- and volume-based geometric standard deviations of the size distribution at three constant average shear rates, G. As flocculation broadens the size distribution, σ_g reaches a maximum and then decreases to an asymptotic value at steady state.

an initial lag period, the number-based geometric standard deviation, σ_{gn}, increases as the distribution broadens into the larger size classes (Figure 1a). A maximum value is reached (e.g., $\sigma_g = 3.27$ at $\tau = 15$ for $G = 10$ s^{-1}) corresponding to the maximum displacement of the larger mode from the primary particle mode of the distribution. As the primary particles are depleted (Figure 1a), σ_{gn} decreases until leveling off at an asymptotic value, σ_{gnss}, corresponding to the attainment of the steady-state size distribution ($\sigma_{gnss} = 2.22$ at $\tau = 28$ for $G = 10$ s^{-1}).

Increasing the shear rate, G, results in an increased fragmentation rate (eq 5), preventing further growth of the steady-state particle size distribution. As a result, the steady-state PSD is displaced to smaller sizes and narrowed as the number of primary particles present at steady state is increased compared to the steady-state PSD at lower shear rates (e.g., at $G = 50$ s^{-1} the concentration of primary particles at steady state is $N_{1ss} = 5\%$). This is shown in Figure 2 where σ_{gnss} decreases with increasing G. Furthermore, the maximum in σ_{gn} decreases with increasing G since the two size modes (primary particles and flocs) become increasingly indistinguishable. For example, the primary particle concentration at steady state is 5% for $G = 50$ s^{-1} and becomes 18% for $G = 100$ s^{-1} (Spicer and Pratsinis, 1996a).

Figure 2 also shows the evolution of the geometric standard deviation, σ_{gv}, of the corresponding volume-based PSD. A rapid increase in σ_{gv} is initially observed as the distribution broadens and larger particles are formed (Figure 1b). As with the number-based PSD, a maximum is reached, corresponding to the maximum separation of the primary particle and floc modes. At a constant G, the maximum σ_{gv} is smaller than the maximum σ_{gn} because of the larger relative contribution of the primary particles to the number- versus the volume-based PSD. At the employed shear rates the primary particles contribute little to the latter distribution, so the same σ_{gv} is attained at all shear rates. The steady-state σ_{gv} is unchanged by the shear rate, consistent with Spicer and Pratsinis (1996b), who found that shear does not change the width of the polystyrene floc size distribution at steady state, so it is self-preserving with respect to shear.

Figure 3 shows the steady-state geometric standard deviation for the number- and volume-based PSD (σ_{gnss}

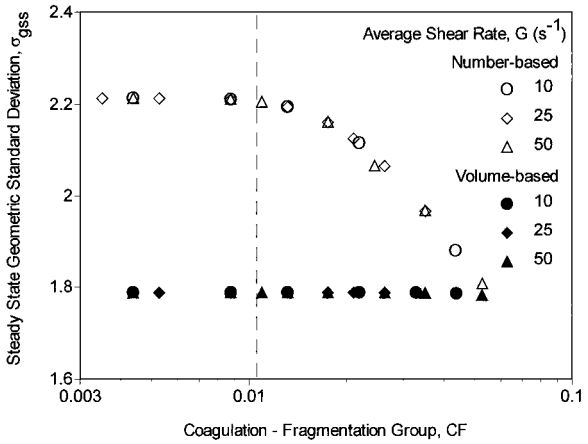

Figure 3. Steady-state number- (open symbols) and volume-based (filled symbols) geometric standard deviations, σ_{gnss} and σ_{gvss}, as a function of the coagulation−fragmentation group CF for various shear rates G. σ_{gss} increases as CF decreases, allowing flocculation to broaden the size distribution. An asymptotic value is reached below a critical value of CF, indicating a self-preserving steady-state PSD that includes very few primary particles (broken line: $N_{1ss} < 0.01N_T$).

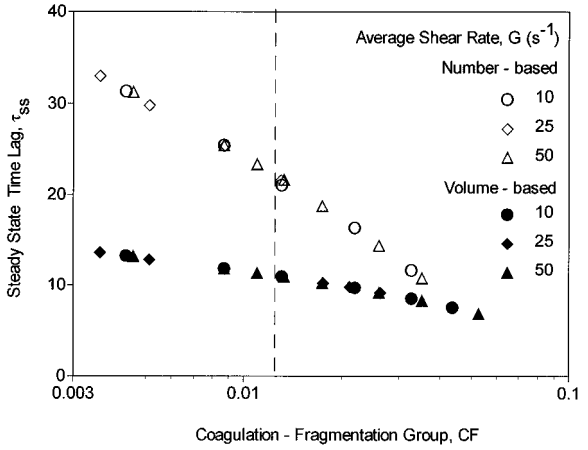

Figure 4. Steady-state time lag for the number- (open symbols) and volume-based (filled symbols) PSDs as a function of CF. Increasing the significance of fragmentation decreases the time lag for steady-state attainment by limiting the development of the PSD. When scaled by CF, the time lag data collapse onto two universal lines independent of the degree of development of the steady-state size distribution.

and σ_{gvss}, respectively) as a function of the coagulation−fragmentation group, CF, for various shear rates G and breakup coefficients A. In Figure 3, all values of σ_{gnss} and σ_{gvss} collapse onto a single curve when scaled by the dimensionless parameter CF. This indicates that a universal asymptotic behavior is exhibited by a coagulation−fragmentation system for this combination of rate expressions. In Figure 3, σ_{gnss} increases and approaches an asymptotic value of 2.22 with decreasing values of CF. This asymptotic behavior is indicative of the self-preserving properties of the fully developed steady-state PSD (Spicer and Pratsinis, 1996a,b). Increasing the CF corresponds to increased fragmentation relative to coagulation, causing σ_{gnss} to decrease from its value when fully-developed ($N_{1ss} \leq 0.01N_{Tss}$, where N_{Tss} is the total number concentration present at steady state). This is attributed to the narrowing of the size distribution as increased fragmentation shifts the distribution to the smallest sections. The threshold CF (1% from the asymptotic CF) corresponding to $N_{1ss} \leq 0.01N_T$ is CF = 0.013. Figure 3 also shows the effect of CF on σ_{gvss}. Here also, increasing CF slightly decreases σ_{gvss} below the self-preserving $\sigma_{gvss} = 1.79$. The effect of increased fragmentation rates is smaller for the volume-based than for the number-based PSD because of the sensitivity of the latter distribution to the dynamics of the primary particles. This is seen in Figure 3 as a significant decrease in σ_{gnss} to the right of the dotted line, indicating the number fraction of the smallest particles exceeding 1%. For the volume distribution, the deviation of σ_{gvss} from self-similarity occurs when $V_{1ss} \geq 0.01V_{Tss}$ (where V_{Tss} is the total solids volume present at steady state).

The dynamics of the floc size distribution can be quantitatively characterized through the evolution of σ_{gn} and σ_{gv} of the distribution (Figure 2). In addition, σ_g is readily measured by light-scattering techniques and is used as a measure of product particle quality in numerous industrial processes. Thus, σ_g provides a practical and theoretical criterion for the attainment of steady state and thus the time lag before attainment of steady state. By analogy with previous work on Brownian coagulation (Vemury et al., 1994), the criterion for the attainment of steady state was defined as the dimensionless time (τ_{ss}) at which the distribution was within 1% of its steady-state σ_g. Figure 4 shows the steady-state time lag, τ_{ss}, for the number (τ_{nss}) and volume (τ_{vss}) distributions as a function of CF. As in Figure 3, τ_{ss} values collapse onto a single curve for the number- and volume-based PSD when scaled with CF. Linear regression gives

$$\tau_{nss} = -22.35 \log \mathrm{CF} - 20.69$$

$$\tau_{vss} = -5.60 \log \mathrm{CF} + 0.496 \qquad (9)$$

At low CF, a large difference between τ_{nss} and τ_{vss} is observed. Lower values of CF correspond to increased collision rates for small particles (eq 8). As a result, the size distribution is able to develop into larger sizes before fragmentation halts its progress. Increasing the CF decreases τ_{ss} for both number and volume distributions as a result of the increased fragmentation rates and the resulting decreased extent of PSD development. It is interesting to note that the scaling of τ_{ss} is unchanged by a deviation from the self-preserving σ_g of the steady-state size distribution (i.e., the values of τ_{ss} collapse onto a single curve even to the right of the broken line, indicating the point of deviation from the self-preserving size distribution). τ_{nss} is significantly larger than τ_{vss} as a result of the larger effect of the primary particle dynamics on steady-state attainment by the number-based PSD.

Effect of Shear Rate Fluctuations on the Attainment of Steady State. Equation 4 is a simplified description of the variation of the instantaneous shear rate within the turbulent flow field of the stirred tank. This description is based on the concept of an average circulation time for a suspended particle or fluid element (Oldshue, 1984; Kim and Glasgow, 1987). Particles are exposed to a spectrum of shear rates during the flocculation process. For example, fluid elements start from a region of say, average G, reach the region of maximum G at the impeller zone, then reach the relatively stagnant region above the impeller, and finally return back to the high shear impeller zone. This is consistent with the flow pattern for a radial flow impeller such as a Rushton configuration (Holland and Chapman, 1966). Increasing the amplitude of the shear rate fluctuation, ω, increases the range of G experienced by the sus-

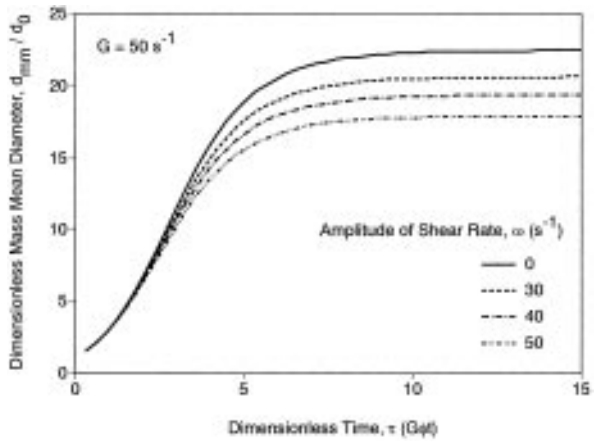

Figure 5. Evolution of the dimensionless mass mean diameter as a function of the maximum amplitude of the fluctuation in G, ω. The mean floc size increases during the growth-dominated regime and then levels off once steady state is attained. Increased ω decreases the steady-state value as a result of increased fragmentation.

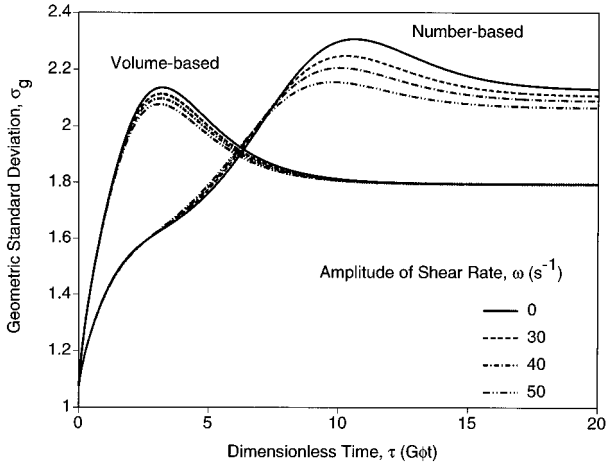

Figure 6. Evolution of the number- and volume-based geometric standard deviation of the size distribution as a function of the amplitude of the spatially averaged shear rate, G. Larger amplitudes increase fragmentation, suppressing the development of the size distribution and thus decreasing its width.

pended particles. The shear rate variation for the four cases examined in this study were $G = 50$ s^{-1} and $\omega = 0$, 30, 40, and 50 s^{-1}.

Figure 5 shows the evolution of the dimensionless mass mean floc diameter (Hinds, 1982), d_{mm}/d_0, at various shear rate amplitudes. During the growth-dominated region of flocculation, d_{mm} increases rapidly as shear-induced collisions promote particle growth. As larger particles are formed, the significance of fragmentation increases, the particle growth rate slows down, and d_{mm} levels off so a steady state is reached ($\tau = 8$ at $\omega = 0$ as in Figures 1−3). It is interesting to note that the system reaches a stable steady state (with small oscillations) despite the large variance in the value of G, consistent with experimental data (Reich and Vold, 1959; Oles, 1992; Spicer and Pratsinis, 1996b). Increasing ω slows the growth of d_{mm}, resulting in smaller particles at steady state. Exposure of the flocs to larger shear rates at higher G amplitudes increases their fragmentation rate, providing a greater contribution of fragmentation to the attainment of steady state. During the later stages of flocculation the role of fragmentation in steady-state attainment is significant, so the largest values of G restrict floc growth.

Figure 5 showed that the evolution of the PSD and the average floc size are influenced by fluctuations in the shear rate. Figure 6 shows the effect of ω on the evolution of σ_g for $G = 50$ s^{-1}. In Figure 6, σ_{gn} follows the trend observed in Figure 2: the distribution width increases initially, reaches a maximum, and then descends to its steady-state value. Increasing ω slightly accelerates the initial ($\tau < 10$) increase in σ_{gn} relative to the case of constant shear as a result of the strong dependence of the collision frequency of the larger particles on shear rate (eq 2). The second mode of the distribution forms more rapidly with increasing shear rate amplitude, thus accelerating the rate of increase by σ_{gn}. Once fragmentation becomes significant, however, the larger fluctuations in G significantly suppress the growth of larger particles, reducing the maximum σ_{gn} (Figure 6). The steady-state value of σ_{gn} is decreased slightly by increasing the amplitude of the shear fluctuations since the fraction of the primary particles increases (e.g., for $\omega = 0$, $N_{1ss} = 5\%$, while for $\omega = 50$ s^{-1}, $N_{1ss} = 8\%$). When the progress of the distribution is halted at lower sizes by fragmentation, the steady-state distribution will be narrower (Spicer and Pratsinis, 1996b) with a corresponding decrease in σ_{gn}.

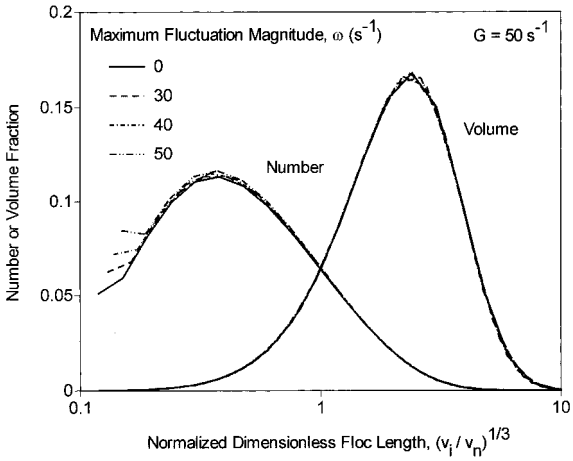

Figure 7. Effect of ω on the shape of the self-preserving steady-state floc number and volume distributions. The steady-state number-based PSD narrows as a result of the increased fragmentation at higher ω, but the volume-based PSD does not since primary particles contribute less to the latter PSD.

The effect of increasing ω is smaller for σ_{gv} than for σ_{gn} but similar: the maximum σ_g reached decreases as the shear fluctuations increase in magnitude. This reflects the restriction of floc growth into the larger sizes, producing a distribution of smaller relative particle sizes (Figure 5). As for the case of $\omega = 0$, however, the distribution is able to fully develop before fragmentation balances growth completely. As a result, σ_{gvss} changes very little with respect to ω. The fluctuation of G shifts the steady-state PSD into the lower sizes (Figure 5) but does not significantly influence its shape since the contribution of the primary particles to the steady-state volume-based PSD is very small.

The results in Figure 6 indicate the importance of shear fluctuations on the development of the PSD. The asymptotic behavior of the system is also affected by the fluctuations. Figure 7 shows the steady-state floc number and volume distributions, plotted in normalized form (i.e., v_i normalized by the number-average volume, v_n) to evaluate their self-preserving properties, as a function of ω. In all four number distributions in Figure 7, the large shoulder of the normalized distribution collapses onto a single line. The only deviation from

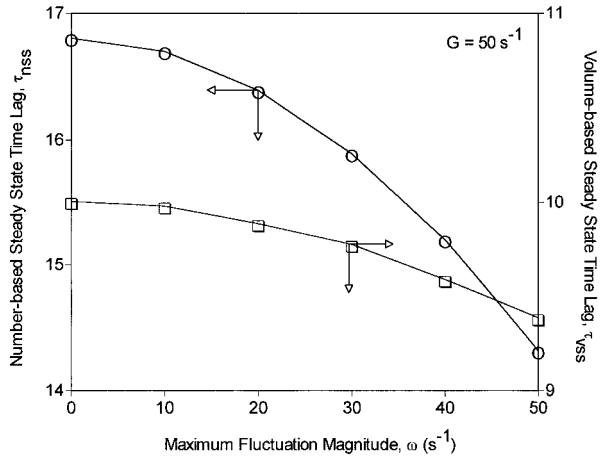

Figure 8. Effect of ω on the time lag for steady-state attainment. Increasing ω decreases both time lags for the number- and volume-based PSD as a result of the increased fragmentation rates and less development of the steady-state PSD.

self-similarity is at the lower size range of the number-based PSD, where restriction of the distribution by fragmentation prevents total depletion of the primary particles (Spicer and Pratsinis, 1996a). Increasing ω accelerates fragmentation, resulting in a larger fraction of primary particles. In Figure 7, full self-similarity of the steady-state floc volume distribution is observed for all ω. Shear fluctuations do not affect the shape of the asymptotic volume distribution when the primary particles contribute less than 1% of the mass of the suspension (Figure 6).

Figure 8 shows the effect of ω on the steady-state time lag for the number and volume distributions. Increasing the amplitude of the shear fluctuations decreases the time required for both distributions to attain steady state, while increased shear decreases the time lag for steady state as the distribution is halted at smaller sizes. As ω is increased, the intensity of fragmentation increases, and the distribution attains steady state more rapidly because less particle growth is possible.

Conclusions

A theoretical model of coagulation and fragmentation has been used to describe shear-induced flocculation. The initially monodisperse size distribution broadens as particles grow by shear-induced coagulation. The width of the size distribution increases initially, passes through a maximum as two particle size modes are formed, and then decreases as the fine size mode is depleted to reach an asymptotic value at steady state. Increased shear rates decrease the number-based σ_g at steady state and to a lesser extent the volume-based σ_g. σ_g is used as a criterion to quantify the attainment of steady state and determine the time lag for attainment of steady state, τ_{ss}. τ_{ss} decreases with increased significance of fragmentation by halting development of the distribution at smaller particle sizes. A dimensionless group, CF, is found that describes the relative significance of coagulation and fragmentation. For CF < 0.013 the steady-state size distribution has fully grown and has a number- or volume-based geometric standard deviation of 2.22 or 1.79, respectively.

The heterogeneous flow field of a stirred tank is simulated using a sinusoidally varying average shear rate. Increasing the shear rate amplitude, ω, decreases the steady-state mass mean floc size and the steady-state time lag, but it does not affect the width of the distribution provided that most primary particles (>99%) have grown into larger particles.

Acknowledgment

This research was supported by Genencor International B.V. and a graduate fellowship from the Quantum Chemical Co.

Literature Cited

Blatz, P. J.; Tobolsky, A. V. Note on the Kinetics of Systems Manifesting Simultaneous Polymerization−Depolymerization Phenomena. *J. Phys. Chem.* **1945**, *49*, 77.

Boadway, J. D. Dynamics of Growth and Breakage of Alum Floc in Presence of Fluid Shear. *J. Environ. Eng. Div. (Am. Soc. Civ. Eng.)* **1978**, *104*, 901.

Clark, M. M. Critique of Camp and Stein's RMS Velocity Gradient. *J. Environ. Eng.* **1985**, *111*, 741.

Cohen, R. D. Self-Similar Cluster Size Distribution in Random Coagulation and Breakup. *J. Colloid Interface Sci.* **1992**, *149*, 261.

Coulaloglou, C. A.; Tavlarides, L. L. Description of Interaction Processes in Agitated Liquid−Liquid Dispersions. *Chem. Eng. Sci.* **1977**, *32*, 1289.

Cutter, L. A. Flow and Turbulence in a Stirred Tank. *AIChE J.* **1966**, *12*, 35.

Danov, K. D.; Ivanov, I. B.; Gurkov, T. D.; Borwankar, R. P. Kinetic Model for the Simultaneous Processes of Flocculation and Coalescence in Emulsion Systems. *J. Colloid Interface Sci.* **1994**, *167*, 8.

Family, F.; Meakin, P.; Deutch, J. M. Kinetics of Coagulation with Fragmentation: Scaling Behavior and Fluctuation. *Phys. Rev. Lett.* **1986**, *57*, 727.

Friedlander, S. K. *Smoke, Dust, and Haze*; Wiley: New York, 1977.

Golovin, A. M. The Solution of the Coagulation Equation for Raindrops, Taking Condensation into Account. *Bull. Acad. Sci. SSSR Geophys. Ser. (Eng. Transl.)* **1963**, 482.

Hinds, W. C. *Aerosol Technology*; Wiley-Interscience: New York, 1982.

Holland, F. A.; Chapman, F. S. *Liquid Mixing and Processing in Stirred Tanks*; Reinhold: London, 1966.

Hounslow, M. J.; Ryall, R. L.; Marshall, V. R. A Discretized Population Balance for Nucleation, Growth, and Aggregation. *AIChE J.* **1988**, *34*, 1821.

IMSL, User's Manual, IMSL Math/Library, Vol. 2, Version 1.1, Houston, 1989.

Kim, Y. H.; Glasgow, L. A. Simulation of Aggregate Growth and Breakage in Stirred Tanks. *Ind. Eng. Chem. Res.* **1987**, *26*, 1604.

Koh, P. T. L.; Andrews, J. R. G.; Uhlerr, P. H. T. Modelling Shear Flocculation by Population Balances. *Chem. Eng. Sci.* **1984**, *42*, 353.

Koh, P. T. L.; Andrews, J. R. G.; Uhlerr, P. H. T. Flocculation in Stirred Tanks. *Chem. Eng. Sci.* **1987**, *39*, 975.

Kusters, K. A. The Influence of Turbulence on Aggregation of Small Particles in Agitated Vessels. Ph.D. Dissertation, Eindhoven University of Technology, Eindhoven, The Netherlands, 1991.

Kusters, K. A.; Pratsinis, S. E.; Thoma, S. G.; Smith, D. M. Ultrasonic Fragmentation of Agglomerate Powders. *Chem. Eng. Sci.* **1993**, *48*, 4119.

Lu, C. F.; Spielman, L. A. Kinetics of Floc Breakage and Aggregation in Agitated Liquid Suspensions. *J. Colloid Interface Sci.* **1985**, *103*, 95.

Meakin, P. Scaling in Aggregation with Breakup Simulations and Mean-Field Theory. *Phys. Rev. Lett.* **1988**, *60*, 2503.

Narsimhan, G.; Ramkrishna, D.; Gupta, J. P. Analysis of Drop Size Distributions in Lean Liquid−Liquid Dispersions. *AIChE J.* **1980**, *26*, 991.

Oldshue, J. Y. *Fluid Mixing Technology*; McGraw-Hill: New York, 1984.

Oles, V. Shear-Induced Aggregation and Breakup of Polystyrene Latex Particles. *J. Colloid Interface Sci.* **1992**, *154*, 351.

Pandya, J. D.; Spielman, L. A. Floc Breakage in Agitated Suspensions: Theory and Data Processing Strategy. *J. Colloid Interface Sci.* **1982**, *90*, 517.

Peled, C. R.; Braun, G.; Nir, S. Time of Equilibration in Reversible Aggregation of Particles. *J. Colloid Interface Sci.* **1995**, *169*, 204.

Peng, S. J.; Williams, R. A. Direct Measurement of Floc Breakage in Flowing Suspensions. *J. Colloid Interface Sci.* **1994**, *166*, 321.

Pulvermacher, B.; Ruckenstein, E. Similarity Solutions of Population Balances. *J. Colloid Interface Sci.* **1974**, *46*, 428.

Reich, I.; Vold, R. D. Flocculation−Deflocculation in Agitated Suspensions. I. Carbon and Ferric Oxide in Water. *J. Phys. Chem.* **1959**, *63*, 1497.

Saffman, P.; Turner, J. On the Collision of Drops in Turbulent Clouds. *J. Fluid Mech.* **1956**, *1*, 16.

Seckler, M. M.; Bruinsma, O. S. L.; Van Rosmalen, G. M. Influence of Hydrodynamics on Precipitation: A Computational Study. *Chem. Eng. Commun.* **1995**, *135*, 113.

Spicer, P. T.; Pratsinis, S. E. Coagulation−Fragmentation: Universal Steady State Particle Size Distributions. *AIChE J.* **1996a**, *42*, 1612.

Spicer, P. T.; Pratsinis, S. E. Shear-Induced Flocculation: The Evolution of the Floc Structure and the Shape of the Size Distribution at Steady State. *Water Res.* **1996b**, *30*, 1049.

Sprow, F. B. Drop Size Distributions in Strongly Coalescing Agitated Liquid−Liquid Systems. *AIChE J.* **1967**, *13*, 995.

Swift, D. L.; Friedlander, S. K. The Coagulation of Hydrosols by Brownian Motion and Laminar Shear Flow. *J. Colloid Interface Sci.* **1964**, *19*, 621.

Tambo, N.; Watanabe, Y. Physical Aspect of Flocculation Process: I. Fundamental Treatise. *Water Res.* **1979**, *13*, 429.

Vemury, S.; Kusters, K. A.; Pratsinis, S. E. Time Lag for Attainment of the Self-Preserving Particle Size Distribution by Coagulation. *J. Colloid Interface Sci.* **1994**, *165*, 53.

Williams, M. M. R. An Exact Solution of the Fragmentation Equation. *Aerosol Sci. Technol.* **1990**, *12*, 538.

Wright, H.; Ramkrishna, D. Factors Affecting Coalescence Frequency of Droplets in a Stirred Liquid−Liquid Dispersion. *AIChE J.* **1994**, *40*, 767.

Received for review December 19, 1995
Revised manuscript received April 15, 1996
Accepted April 16, 1996[⊗]

IE950786N

[⊗] Abstract published in *Advance ACS Abstracts,* August 15, 1996.